Estimating unknown object dynamics
in human-robot manipulation tasks

Denis Ćehajić, Pablo Budde gen. Dohmann, and Sandra Hirche

Abstract— **Knowing accurately the dynamic parameters of a manipulated object is required for common coordination strategies in physical human-robot interaction. Bias in object dynamics results in inaccurately calculated robot wrenches, which may disturb the human during interaction and bias the recognition of the human motion intention. This paper presents an identification strategy of object dynamics for physical human-robot interaction, which allows the tracking of desired human motion and inducing the motions necessary for parameter identification. The estimation of object dynamics is performed online and the estimator minimizes the least square error between the measured and estimated wrenches acting on the object. Identification-relevant motions are derived by analyzing the persistence of excitation condition, necessary for estimation convergence. Such motions are projected in the null space of the partial grasp matrix, relating the human and the robot redundant motion directions, to avoid disturbance of the human desired motion. The approach is evaluated in a physical human-robot object manipulation scenario.**

I. INTRODUCTION

The close interaction of humans and robots in a shared environment and performing tasks collaboratively, poses many challenges. There is a plethora of useful applications, found in industrial, domestic- and service-related areas, including manufacturing, construction, logistics, rehabilitation, search and rescue. Some tasks, such as carrying heavy objects, or handling objects in a constrained environment or in narrow passageways, can be difficult for a robot or human to accomplish alone. Therefore, continuous interaction and cooperation through a physical coupling between humans and robots is indispensable. As the human and the robot are directly coupled, the behavior of the robot directly influences that of the human and vice versa.

The interaction of the robot during cooperation with the human is achieved through a suitable coordination strategy, traditionally achieved through the impedance/admittance control in combination with the object dynamics model (so that the desired motion of the object is realized [1]–[4]). Wrenches to be applied to the object, needed to cause a desired motion, are usually calculated through the inverse dynamics model [2]–[5]. Any bias in the object dynamic parameters, i.e. mass, center of mass, and moments of inertia, results in *incorrectly* calculated robot wrenches, which may disturb the human during interaction or when performing a desired motion [6], and may affect the trust and interaction behavior of the human partner. Furthermore, biased wrenches

D. Ćehajić, P. Budde gen. Dohmann, and S. Hirche are with the Chair of Information-oriented Control, Technical University of Munich, Germany. {denis.cehajic, pablo.dohmann, hirche}@tum.de

affect effort sharing strategies applied in physical human-robot interaction (pHRI) for reducing human effort [2], [3], dexterous handling of objects [2], as well as any coordination strategy necessary for maintaining desired wrenches on the object. Undesired interaction wrenches bias human intention recognition schemes based on interaction wrenches [3]. Since in many real-life pHRI applications the object dynamic parameters are *unknown*, an online identification strategy for estimating object dynamics is required.

The estimation of dynamic parameters of a manipulated object, in a purely robotic context, has received some attention in the past. Related works include single-point robot contact approaches, performed both in an offline [7], [8], and recursive fashion [9], as well as in a cooperative multi-robot setup, moving in a plane [10]. The estimation is usually performed by taking measurements of the end-effector's motion and applied wrenches as an input. However, applying any of the aforementioned methods directly in the pHRI context is not straightforward, since the human partner is dynamically coupled to the robot. There are a few unique challenges arising in parameter estimation in pHRI: (i) the human is usually unaware of the required motion for identification, (ii) the robot solely executing the identification-relevant motion may cause undesired human wrenches and may disturb the human partner, (iii) the desired estimation strategy needs to account for the human presence by simultaneously allowing the human partner to perform a desired motion *while* inducing an identification-relevant motion, necessary for parameter convergence. Our previous work [6] considers the estimation of relative kinematics in pHRI by generating a robot motion for identification around the pose of the human wrist, resulting in minimal human interaction forces. However, only a particular case of static human motion is considered and, in addition, object dynamics need to be incorporated. To the best knowledge of the authors, identifying object dynamics in the context of pHRI, with the human partner, has not yet been investigated.

The main contribution of this paper is an identification approach for pHRI, which achieves the estimation of the unknown object dynamics, while avoiding undesired human interaction wrenches, thus enabling the human partner to perform a desired motion. We model the pHRI task and derive an object dynamics estimator from the underlying physics. The online estimation strategy minimizes the least-square error between the measured and estimated wrenches acting on the object. We derive necessary motions for the estimator convergence and the resulting robot motion such

that the identification-relevant motion is induced by minimally disturbing the human desired motion. The derived strategy enables simultaneous tracking of a human desired motion, while inducing an identification-relevant motion for parameter estimation. The approach is validated in a pHRI object manipulation setting.

The remainder of this paper is structured as follows: Section II models the human-robot object manipulation task and formulates the problem. The estimation of object dynamics is discussed in Section III. The induction of identification-relevant motions is detailed in Section IV. The approach is evaluated in Section V.

Notation: Bold characters denote vectors (lower case) or matrices (upper case). An identity matrix of size $n \times n$ is $\boldsymbol{I}_n$, $\boldsymbol{0}_n$ is a $n \times n$ matrix with all zero elements. The transpose of a matrix $\boldsymbol{A}$ is $\boldsymbol{A}^T$. The Moore-Penrose pseudoinverse of a non-square matrix $\boldsymbol{A}$ is $\boldsymbol{A}^+$. The $n \times n$ skew-symmetric matrix of a vector $\boldsymbol{a}$ is denoted as $[\boldsymbol{a}]_\times$. All values are expressed in the world frame unless explicitly noted differently. The notation $SE(3)$ denotes the special Euclidean group, $SO(3)$ the special orthogonal group, $se(3)$ the Lie Algebra, and S^3 the unit quaternions.

II. MODELING COOPERATIVE MANIPULATION TASKS

We consider a task where a human and a robot cooperatively manipulate a rigid object in $SE(3)$ with unknown object dynamics as depicted in Fig. 1. More precisely, a tracking problem for the task, where the objective is to manipulate an object from an initial to a desired pose, is being addressed. As an example, the human trajectory is planned and then displayed to the human partner as in [2], [3] or the human trajectory is learned as in [11] (and appropriately transformed to the object frame considering the relative kinematics between the frames). Given a desired object trajectory, a robot motion is to be derived, which tracks such trajectory, imposed by a human partner, and induces motions on the object such that the unknown object dynamics is identified. It is assumed that the dimensionality of the inputs is greater than the dimensionality of the task, i.e. the task is controllable and at least some inputs are redundant, which commonly arises in joint object manipulation [2].
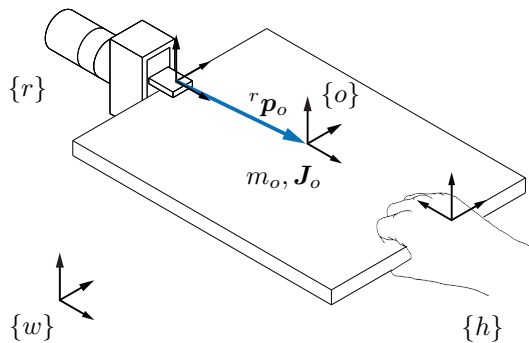
Fig. 1: Cooperative human-robot object manipulation task: Object dynamics is parametrized with the mass m_o, the center of mass $^r\boldsymbol{p}_o$, and the inertia matrix $\boldsymbol{J}_o$.

Coordinate frames of the human, robot, and object are denoted with $\{h\}$, $\{r\}$, and $\{o\}$, respectively. The object frame coincides with the object's center of mass. All coordinate frames are fixed. The pose is represented by $\boldsymbol{x}_i = [\boldsymbol{p}_i^T, \boldsymbol{q}_i^T]^T \in SE(3)$ $\forall i \in h, r, o$ containing the human, robot, and object translation $\boldsymbol{p}_i \in \mathbb{R}^3$ expressed in the world/inertial frame $\{w\}$, and orientation $\boldsymbol{q}_i \in S^3$ represented by a unit quaternion, i.e. $\boldsymbol{q}_i = [\eta_i, \boldsymbol{\epsilon}_i^T]^T$, with $\eta_i \in \mathbb{R}$ as the real part and $\boldsymbol{\epsilon}_i = [\epsilon_{i1}, \epsilon_{i2}, \epsilon_{i3}]^T \in \mathbb{R}^3$ as the imaginary part of the quaternion. A rotation matrix $\boldsymbol{R}(\boldsymbol{q}_i) \in SO(3)$ is given by $\boldsymbol{R}(\boldsymbol{q}_i) = (\eta_i^2 - \boldsymbol{\epsilon}_i^T\boldsymbol{\epsilon}_i)\boldsymbol{I}_3 + 2\boldsymbol{\epsilon}_i\boldsymbol{\epsilon}_i^T + 2\eta_i[\boldsymbol{\epsilon}_i]_\times$. Let $\dot{\boldsymbol{x}}_i = [\boldsymbol{v}_i^T, \boldsymbol{\omega}_i^T]^T \in se(3)$ be a twist vector containing the translational velocity $\boldsymbol{v}_i \in \mathbb{R}^3$, and the angular velocity $\boldsymbol{\omega}_i \in \mathbb{R}^3$, and let $\ddot{\boldsymbol{x}}_i = [\dot{\boldsymbol{v}}_i^T, \dot{\boldsymbol{\omega}}_i^T]^T$ contain translational and angular accelerations.

The dynamics of the object is given by

$$\boldsymbol{M}_o\ddot{\boldsymbol{x}}_o + \boldsymbol{C}_o(\boldsymbol{x}_o, \dot{\boldsymbol{x}}_o) = \boldsymbol{u}_o \ , \tag{1}$$

with $\boldsymbol{u}_o$ as the total object wrenches (defined subsequently), $\boldsymbol{M}_o \in \mathbb{R}^{6\times6}$ as the object inertia and mass matrix, and $\boldsymbol{C}_o \in \mathbb{R}^6$ containing the gravitational and Coriolis effects of the motion

$$\boldsymbol{M}_o = \begin{bmatrix} m_o\boldsymbol{I}_3 & \boldsymbol{0}_3 \\ \boldsymbol{0}_3 & \boldsymbol{J}_o \end{bmatrix} \quad \text{and} \quad \boldsymbol{C}_o = \begin{bmatrix} -m_o\boldsymbol{g} \\ \boldsymbol{\omega}_o \times \boldsymbol{J}_o\boldsymbol{\omega}_o \end{bmatrix} \ , \tag{2}$$

where $m_o \in \mathbb{R}$ is the mass of the object, $\boldsymbol{J}_o \in \mathbb{R}^{3\times3}$ is the symmetric inertia matrix, and $\boldsymbol{g} \in \mathbb{R}^3$ is the gravity vector. For convenience, let us define the parameter vector $\boldsymbol{\theta} \in \mathbb{R}^{10}$ containing all dynamic parameters of the object

$$\boldsymbol{\theta} = [m_o, m_o{}^r\boldsymbol{p}_o^T, {}^r\boldsymbol{J}_o']^T \ , \tag{3}$$

where $^r\boldsymbol{p}_o \in \mathbb{R}^3$ is the vector of the object's center of mass, as depicted in Fig. 1, and $^r\boldsymbol{J}_o'$ is the vector containing six components of the inertia matrix expressed in $\{r\}$, i.e. $^r\boldsymbol{J}_o' = [^rJ_{o_{xx}}, {}^rJ_{o_{xy}}, {}^rJ_{o_{xz}}, {}^rJ_{o_{yy}}, {}^rJ_{o_{yz}}, {}^rJ_{o_{zz}}]$.

The object dynamics (1) expresses the total object wrenches $\boldsymbol{u}_o = [\boldsymbol{f}_o^T, \boldsymbol{t}_o^T]^T$, with $\boldsymbol{f}_o \in \mathbb{R}^3$ as the force and $\boldsymbol{t}_o \in \mathbb{R}^3$ as the torque acting on the object. Wrenches $\boldsymbol{u}_o$ are a result of individual human and robot wrenches accounting for relative kinematics, expressed as

$$\boldsymbol{u}_o = \boldsymbol{G} \begin{bmatrix} \boldsymbol{u}_r \\ \boldsymbol{u}_h \end{bmatrix} \ , \tag{4}$$

where $\boldsymbol{u}_i = [\boldsymbol{f}_i^T, \boldsymbol{t}_i^T]^T \in \mathbb{R}^6$ $\forall i = r, h$ are the wrenches of each partner applied at the grasping point, and $\boldsymbol{G} \in \mathbb{R}^{6\times12}$ is the grasp matrix [1] containing the kinematic constraints of both human and robot frames, with respect to the object frame, given by

$$\boldsymbol{G} = [^o\boldsymbol{G}_r \ {}^o\boldsymbol{G}_h] = \begin{bmatrix} \boldsymbol{I}_3 & \boldsymbol{0}_3 & \boldsymbol{I}_3 & \boldsymbol{0}_3 \\ [^o\boldsymbol{p}_r]_\times & \boldsymbol{I}_3 & [^o\boldsymbol{p}_h]_\times & \boldsymbol{I}_3 \end{bmatrix} \ , \tag{5}$$

with $^o\boldsymbol{G}_i \in \mathbb{R}^{6\times6}$ $\forall i = r, h$ being the partial grasp matrix, and $^o\boldsymbol{p}_i \in \mathbb{R}^3$ the vector from the object frame $\{o\}$ to each grasping point.

Inconsistent robot motion, i.e. robot motion that does not match the human motion, causes undesired interaction wrenches, which disturb the human during interaction. The

human dynamics model suggests that the human applies a wrench $\boldsymbol{u}_h$ when there is a difference between the desired and the actual human motion. As an example, the difference between the desired and the actual human pose can be related to the human wrenches by the model [12]

$$\boldsymbol{K}_h(\boldsymbol{x}_h^d - \boldsymbol{x}_h) = \boldsymbol{u}_h \ , \tag{6}$$

where $\boldsymbol{x}_h^d$ and $\boldsymbol{x}_h$ denote the desired and actual motion of the human, and $\boldsymbol{K}_h \in \mathbb{R}^{6 \times 6}$ contains the translational and rotational stiffness of the human wrist. According to (6), it can be inferred that zero human wrench, i.e. $\boldsymbol{u}_h = 0$, indicates a zero difference between the desired and actual human pose, i.e. $\boldsymbol{x}_h^d = \boldsymbol{x}_h$.

The objective of this work is to estimate the unknown object dynamics such that the parameter estimate $\hat{\boldsymbol{\theta}}$ converges to the true value of the parameter, $\boldsymbol{\theta}$, i.e.

$$\hat{\boldsymbol{\theta}} \to \boldsymbol{\theta} \ . \tag{7}$$

Identification of the object dynamic parameters in the sense of (7) is achieved only if the object motions are sufficiently exciting [13]. Performing such motion might cause undesired human interaction wrenches (6) and might disturb the human when performing a desired motion.

The objective is to perform identification-relevant motions, such that the difference to the human desired motion is minimal. According to (6), this is equivalently expressed as

$$\min_{x_r} ||\boldsymbol{u}_h||^2 \ . \tag{8}$$

We will derive an online object dynamics estimator, such that the parameter estimation objective (7) is achieved. Subsequently, we propose a suitable identification strategy considering objective (8).

III. ESTIMATION OF UNKNOWN OBJECT DYNAMICS

In this section we aim at formulating an estimator of the object dynamics. After introducing necessary kinematics expressions, we derive an object dynamics estimator and provide a detailed convergence discussion, which is required for deriving an identification-relevant motion.

A. Manipulation task kinematics

Since the object is rigid and all grasps are assumed to be fixed, the object constrains the translational and rotational motion of the human and the robot. Namely, the relative kinematics is constant and it is expressed as

$$^o\boldsymbol{p}_i = \text{const.} \quad \text{and} \quad ^o\boldsymbol{q}_i = \text{const.} \quad \forall i = r, h \tag{9}$$

with $^o\boldsymbol{p}_i \in \mathbb{R}^3$ as the relative displacement, and $^o\boldsymbol{q}_i$ as the relative orientation of $\{h\}$ or $\{r\}$ with respect to $\{o\}$.

Remark: In this work, the relative kinematics between the robot and the human is assumed known and the frames are fixed. Through our previous work [6], it is possible to incorporate online estimation of relative kinematics (quantities in (9)) into the presented approach as well, to account for grasp changes (and/or re-grasping) and slippages of the human hand during interaction.

The position of the human or the robot, with respect to the object expressed in the world frame $\{w\}$, is

$$\boldsymbol{p}_i = \boldsymbol{p}_o + \boldsymbol{R}(^w\boldsymbol{q}_o)^o\boldsymbol{p}_i \quad \forall i = r, h \tag{10}$$

Differentiating (10), we obtain expressions of the kinematics at the velocity level

$$\boldsymbol{v}_i = \boldsymbol{v}_o + \boldsymbol{\omega}_o \times {}^o\boldsymbol{p}_i \tag{11}$$
$$\boldsymbol{\omega}_i = \boldsymbol{\omega}_o \ , \tag{12}$$

and by further differentiation of eqs. (11) and (12) at the acceleration level

$$\dot{\boldsymbol{v}}_i = \dot{\boldsymbol{v}}_o + \dot{\boldsymbol{\omega}}_o \times {}^o\boldsymbol{p}_i + \boldsymbol{\omega}_o \times (\boldsymbol{\omega}_o \times {}^o\boldsymbol{p}_i) \tag{13}$$
$$\dot{\boldsymbol{\omega}}_i = \dot{\boldsymbol{\omega}}_o \ . \tag{14}$$

In general, velocities between any desired frames, can be represented in the compact form as $\dot{\boldsymbol{x}}_i = {}^i\boldsymbol{G}_j^T\dot{\boldsymbol{x}}_j$, e.g. between the robot and the human, as follows

$$\dot{\boldsymbol{x}}_r = \begin{bmatrix} \boldsymbol{I}_3 & -[^h\boldsymbol{p}_r]\times \\ \boldsymbol{0}_3 & \boldsymbol{I}_3 \end{bmatrix} \dot{\boldsymbol{x}}_h = {}^r\boldsymbol{G}_h^T\dot{\boldsymbol{x}}_h \ . \tag{15}$$

B. Estimation model for the object dynamics

We proceed to derive an estimation model of object dynamics in $SE(3)$, based on the underlying physics between the interacting partners. Let us express (4) with respect to $\{r\}$ by accounting for the relative kinematics obtaining

$$^r\boldsymbol{u}_o = \begin{bmatrix} ^r\boldsymbol{f}_o \\ ^r\boldsymbol{t}_o \end{bmatrix} = \begin{bmatrix} \boldsymbol{I}_6 & ^r\boldsymbol{G}_h \end{bmatrix} \begin{bmatrix} \boldsymbol{u}_r \\ \boldsymbol{u}_h \end{bmatrix} \ , \tag{16}$$

with $^r\boldsymbol{G}_h$ as in (15). Following the derivations in the Appendix, this yields the estimation model

$$^r\boldsymbol{u}_o = \begin{bmatrix} \boldsymbol{I}_6 & ^r\boldsymbol{G}_h \end{bmatrix}^+ \boldsymbol{\phi} \, \boldsymbol{\theta} \ , \tag{17}$$

with $\boldsymbol{\phi} \in \mathbb{R}^{6 \times 10}$ as the regressor matrix

$$\boldsymbol{\phi} = \begin{bmatrix} \dot{\boldsymbol{v}}_r - {}^r\boldsymbol{g} & [\dot{\boldsymbol{\omega}}_o]_\times + [\boldsymbol{\omega}_o]_\times[\boldsymbol{\omega}_o]_\times & \boldsymbol{0}_{3 \times 6} \\ \boldsymbol{0}_{3 \times 1} & [^r\boldsymbol{g} - \dot{\boldsymbol{v}}_r]_\times & [.\dot{\boldsymbol{\omega}}_o] + [\boldsymbol{\omega}_o]_\times[.\boldsymbol{\omega}_o] \end{bmatrix}, \tag{18}$$

and $\boldsymbol{\theta}$ as the vector of unknown dynamic parameters as in (3), and matrices $[.\dot{\boldsymbol{\omega}}_o]$ and $[.\boldsymbol{\omega}_o]$ both $\in \mathbb{R}^{3 \times 6}$, as defined in the Appendix (31). The gravity vector is defined as $\boldsymbol{g} = [0, 0, -9.81]^T$ (m/s²), with a single negative component along the z-axis, and $^r\boldsymbol{g} = \boldsymbol{R}(^r\boldsymbol{q}_w)\boldsymbol{g}$, accounting for rotation with respect to $\{w\}$. It is straightforward to see from (17) that the model is linear in the unknown object dynamics parameters.

Remark: The human presence during interaction is accounted for in the model (17) through: (i) the induced human wrench $\boldsymbol{u}_h$ contained in $^r\boldsymbol{u}_o$, (ii) the angular motion constrained by the object, i.e. $\boldsymbol{\omega}_o = \boldsymbol{\omega}_h$ and $\dot{\boldsymbol{\omega}}_o = \dot{\boldsymbol{\omega}}_h$ (c.f. eqs. (12) and (14)), and (iii) the relative kinematics between the human and the robot in (15).

Note that any number of human and robotic partners can be incorporated into the model (17), by appropriately including agents' end-effectors' wrenches acting on the object in (16), and accounting for the relative kinematics.

C. Online object dynamics estimator

Having introduced the estimation model (17), we formulate an *online* estimator of the unknown object dynamic parameters $\boldsymbol{\theta}$. Measurements are acquired at each $k\Delta t$, with k as the discrete time index and Δt as the sampling time interval. Input to the estimator are measurements (the superscript k denotes the discrete time instant): of the wrenches acting on the object $^r\boldsymbol{u}_h^k$, the robot translational acceleration $\dot{\boldsymbol{v}}_r^k$, the object angular velocity and acceleration, $\boldsymbol{\omega}_o^k$ and $\dot{\boldsymbol{\omega}}_o^k$. A discussion how those measurements are obtained, is found in Section V.

Let $\hat{\boldsymbol{\theta}}^k$ denote an estimate of object dynamic parameters at each k. Given the aforementioned measurements and $\hat{\boldsymbol{\theta}}$, estimated wrenches acting on the object, $^r\hat{\boldsymbol{u}}_o$, are computed through the model (17). An optimization problem, solving for unknown dynamics, can be formulated in terms of least squares. Let us define the cost function as

$$\min_\theta \frac{1}{2} \sum_{k=1}^K w^k \|\boldsymbol{e}_u^k\|^2 \ , \qquad (19)$$

where $\boldsymbol{e}_u^k \in \mathbb{R}^{12}$ are the wrenches residuals from eq. (17)

$$\boldsymbol{e}_u^k = {}^r\hat{\boldsymbol{u}}_o^k - {}^r\boldsymbol{u}_o^k \ , \qquad (20)$$

being weighted by $w^k \leq 1 \ \forall k = 1, 2, \ldots, K$, with K as the measurement horizon.

The recursive least square estimator [13] is used for estimating the unknown $\boldsymbol{\theta}$. The update of the object dynamics estimator minimizing (19) is given by

$$\hat{\boldsymbol{\theta}}^k = \hat{\boldsymbol{\theta}}^{k-1} + \boldsymbol{K}^k \boldsymbol{e}_u^k \ , \qquad (21)$$

with the error $\boldsymbol{e}_u^k$ as in (20), considering only measurements at k, the gain $\boldsymbol{K}^k \in \mathbb{R}^{10\times6}$ and matrix $\boldsymbol{P}^k \in \mathbb{R}^{10\times10}$ as

$$\boldsymbol{K}^k = \boldsymbol{P}^{k-1} (\boldsymbol{\phi}^k)^T (\delta\boldsymbol{I}_6 + \boldsymbol{\phi}^k \boldsymbol{P}^{k-1}(\boldsymbol{\phi}^k)^T)^{-1}$$
$$\boldsymbol{P}^k = \frac{1}{\delta}(\boldsymbol{I}_6 - \boldsymbol{K}^k\boldsymbol{\phi}^k)\boldsymbol{P}^{k-1} \ ,$$

with the initial estimates $\hat{\boldsymbol{\theta}}^0$ and $\boldsymbol{P}^0$, and the weight δ as the forgetting factor defined between $0 < \delta \leq 1$. Note that $\boldsymbol{P}^0$ is either set to $\boldsymbol{P}^0 = ((\boldsymbol{\phi}^0)^T\boldsymbol{\phi}^0)^{-1}$, where $(\boldsymbol{\phi}^0)^T\boldsymbol{\phi}^0$ is non-singular, or in the case of high initial uncertainty, the elements of $\boldsymbol{P}^0$ are set to high values; δ typically uses values $0.95 < \delta < 1$: the closer the value is to 1, the less data is being forgotten resulting in increased estimation stability and reduced estimation adjustments [14], increasing the estimator's rate of convergence.

Remark: Any other recursive estimator can be used for estimating $\hat{\boldsymbol{\theta}}$, such as the total least square as in [9] or gradient descent [13]. Furthermore, it is also possible to directly account for sensor noise in the model (17).

D. Estimator convergence

The estimator (21) converges to the true dynamic parameters if the input motions satisfy the persistence of excitation (PE) condition [13]. When satisfied, the system inputs are sufficiently "rich" for identifying the unknown parameters of object dynamics. Formally, the estimate of object dynamics $\hat{\boldsymbol{\theta}}$ converges to $\boldsymbol{\theta}$ if

$$\int_t^{t+T} \boldsymbol{\phi}^T\boldsymbol{\phi} \ d\tau \geq \alpha\boldsymbol{I}_{10} \ , \qquad (22)$$

is satisfied for some constants $T > 0$, $\alpha > 0 \ \forall t$, with $\boldsymbol{\phi}$ being the regressor matrix as in (18). Relation (22) implies that the PE condition is satisfied if the integral of $\boldsymbol{\phi}^T\boldsymbol{\phi}$ over the time interval $[t, t + T]$ is positive definite. Accordingly, the observability of $\boldsymbol{\theta}$ depends on the object's angular motions $\boldsymbol{\omega}_o$ and $\dot{\boldsymbol{\omega}}_o$, and the robot's translational acceleration $\dot{\boldsymbol{v}}_r$, contained in $\boldsymbol{\phi}$ in (18). We observe:

(i) If all measurements $\boldsymbol{\omega}_o, \dot{\boldsymbol{\omega}}_o, \dot{\boldsymbol{v}}_r$ are zero $\forall t$, which occurs when the human and the robot hold the object statically, the matrix product $\boldsymbol{\phi}^T\boldsymbol{\phi}$ is positive semidefinite and condition (22) is not satisfied. Still, the parameter m_o and the components $^rp_{o,x}$, $^rp_{o,y}$ of $^r\boldsymbol{p}_o$ in (3) are already observable from the relation $\dot{\boldsymbol{v}}_r - {}^r\boldsymbol{g}$ in (17). Unobservable parameters are $^rp_{o,z}$ and $\boldsymbol{J}_o$.

(ii) If there exists $t_1, t_2 \in [t, t + T]$, such that $\dot{\boldsymbol{v}}_r(t_1) \neq \dot{\boldsymbol{v}}_r(t_2)$ and $\dot{\boldsymbol{v}}_r(t) \neq \boldsymbol{g}$, $\boldsymbol{\omega}_o(t) = 0$ for $t = t_1, t_2$, the product $\boldsymbol{\phi}^T\boldsymbol{\phi}$ is positive semidefinite and condition (22) is not satisfied; parameters m_o and $^r\boldsymbol{p}_o$ are observable (the component $^rp_{o,z}$ of $^r\boldsymbol{p}_o$ becomes observable), whereas $\boldsymbol{J}_o$ is unobservable.

(iii) If there exists $t_1, t_2 \in [t, t + T]$, such that $\boldsymbol{\omega}_o(t_1) \neq \boldsymbol{\omega}_o(t_2)$ and $\dot{\boldsymbol{v}}_r(t) = 0$ for $t = t_1, t_2$, the matrix product $\boldsymbol{\phi}^T\boldsymbol{\phi}$ is positive definite and condition (22) is satisfied, *all* parameters $\boldsymbol{\theta}$ are observable.

This implies that non-collinear angular motions within an identification horizon T achieve the complete observability of parameters $\boldsymbol{\theta}$. Therefore, in the following we focus on angular motions as the identification-relevant motions.

Remark: An angular motion around a single axis of rotation identifies a subspace of the parameters, e.g. when $w_{o,y}(t) = w_{o,z}(t) = 0$ and $w_{o,x}(t)$ satisfies (22), in addition to m_o and $^r\boldsymbol{p}_o$, the components of the inertia vector related to x-axis are observable. The components $J_{o_{xx}}, J_{o_{xy}}$ and $J_{o_{xz}}$ of $\boldsymbol{J}_o$ are identifiable through the matrix product $[.\dot{\boldsymbol{\omega}}_o] + [\boldsymbol{\omega}_o]_\times[.\boldsymbol{\omega}_o]$ contained in (18).

Inducing identification-relevant motions solely might disturb the human (6), contradicting objective (8), which requires consideration of an appropriate strategy as discussed in the following section.

IV. IDENTIFICATION WITH THE HUMAN-IN-THE-LOOP

We derive an appropriate robot motion which induces identification-relevant motions. By analyzing input redundancies and defining redundant and non-redundant directions between the cooperants, a suitable identification strategy avoiding undesired human interaction wrenches is derived.

A. Input dimensionalities and redundancies

During interaction between the human and the robot, both partners do not necessarily apply wrenches along all

directions. Let us define object wrenches in (4) as

$$\boldsymbol{u}_o = \bar{\boldsymbol{G}}\bar{\boldsymbol{u}} = \begin{bmatrix} {}^o\bar{\boldsymbol{G}}_r & {}^o\bar{\boldsymbol{G}}_h \end{bmatrix} \begin{bmatrix} \bar{\boldsymbol{u}}_r \\ \bar{\boldsymbol{u}}_h \end{bmatrix} , \qquad (23)$$

where $\bar{\boldsymbol{u}}_i \in \mathbb{R}^{n_i}$ are the applied wrenches of a partner, and ${}^o\bar{\boldsymbol{G}}_i \in \mathbb{R}^{m \times n_i}$ is the partial grasp matrix relating each agent's applied wrenches to object wrenches. The applied wrench of an agent is given by

$$\bar{\boldsymbol{u}}_i = \boldsymbol{S}_i \boldsymbol{u}_i , \qquad (24)$$

with $\boldsymbol{S}_i \in \mathbb{R}^{n_i \times m}$ the selection matrix with elements $s_{ij} = \{0, 1\}$ depending on whether a partner can apply a particular force or torque along the direction or not.

The input dimensionality of each partner is $n_i = \dim(\bar{\boldsymbol{u}}_i) = \operatorname{rank}(\bar{\boldsymbol{G}}_i)$, and $n = n_r + n_h$ is the total input dimensionality of all agents. The dimensionality of the task is $m = \dim(\boldsymbol{u}_o) = \operatorname{rank}(\boldsymbol{G})$. In the case of *no* input redundancy, the intersection of the images of the partial grasp matrices is an empty set, i.e. $\operatorname{im}({}^o\bar{\boldsymbol{G}}_r) \cap \operatorname{im}({}^o\bar{\boldsymbol{G}}_h) = \varnothing$. We address the problem of redundant inputs, as this is commonly encountered in joint manipulation [2]. In this case we can differentiate between the *partial* input redundancy, when the intersection of the images of the partial grasp matrices, i.e. $\operatorname{im}({}^o\bar{\boldsymbol{G}}_r) \cap \operatorname{im}({}^o\bar{\boldsymbol{G}}_h)$, is a non-empty set, and *full* input redundancy, when the images of the partial grasp matrices $\operatorname{im}({}^o\bar{\boldsymbol{G}}_r)$ and $\operatorname{im}({}^o\bar{\boldsymbol{G}}_h)$ are equal.

B. Identification avoiding undesired human wrenches

Robot motions need to account for the human desired motion and induce motions satisfying (22). The expression relating wrenches of the robot and the human in (16) can equivalently be expressed with the partial grasp matrix, ${}^h\bar{\boldsymbol{G}}_r$. The robot applied wrenches $\boldsymbol{u}_r$ consist of the external and internal wrench components, where the external is the motion-inducing component and the internal component results in no motion and it lies in the null space of ${}^h\bar{\boldsymbol{G}}_r$ [1]

$$\operatorname{null}({}^h\bar{\boldsymbol{G}}_r) = \{\bar{\boldsymbol{u}}_r |{}^h\bar{\boldsymbol{G}}_r\bar{\boldsymbol{u}}_r = 0\} . \qquad (25)$$

Let $\dot{\boldsymbol{x}}_r^d$ denote the robot motion necessary for tracking a human desired motion and inducing an identification-relevant motion, if the object motion is not satisfying the PE condition (22). For achieving the objective (8) an optimization problem is formulated such that the cost function

$$\min_{x_r^d} \frac{1}{2} \sum_{i=1}^{k} \|\boldsymbol{u}_h^i\|^2 , \qquad (26)$$

is minimized over $\boldsymbol{x}_r^d$. Instead of directly applying an optimization technique for solving $\boldsymbol{x}_r^d$ and minimizing (26), we address the problem at the velocity level ((15)). In addition, we present a strategy for the case $n_h < n_r$, i.e. when the robot has greater input dimensionality than the human.

Let us then redefine (15) relating the human and the robot velocities as

$$\dot{\boldsymbol{x}}_h^R = {}^h\bar{\boldsymbol{G}}_r^T \dot{\boldsymbol{x}}_r , \qquad (27)$$

where $\dot{\boldsymbol{x}}_h^R \in \mathbb{R}^{n_h}$ is the human motion along the redundant directions. As an example, in the case when the human performs translational motion around all three axes, $\dot{\boldsymbol{x}}_h^R = \boldsymbol{v}_h^T$, and ${}^h\bar{\boldsymbol{G}}_r^T = [\boldsymbol{I}_3 \;\; -[{}^r\boldsymbol{p}_h]_\times]$.

The robot motion $\dot{\boldsymbol{x}}_r^d$ is derived by solving (27) for $\dot{\boldsymbol{x}}_r$. Let any vector $\dot{\boldsymbol{x}}_{\mathrm{id}}$ denote identification-relevant motions and $\bar{\dot{\boldsymbol{x}}}_{\mathrm{id}} \in \mathbb{R}^{n_r - n_h}$ as the identification motions in the directions not spanned by $\dot{\boldsymbol{x}}_h^R$. In relation to $\dot{\boldsymbol{x}}_{\mathrm{id}}$, $\bar{\dot{\boldsymbol{x}}}_{\mathrm{id}}$ is given by $\bar{\dot{\boldsymbol{x}}}_{\mathrm{id}} = \boldsymbol{S}_{\mathrm{id}}\dot{\boldsymbol{x}}_{\mathrm{id}}$, where $\boldsymbol{S}_{\mathrm{id}} \in \mathbb{R}^{(n_r - n_h) \times n_r}$ is the selection matrix with elements $s_{ij} = \{0, 1\}$ depending on whether the human motion spans the particular direction or not.

From eq. (25) it can be inferred that minimal disturbance of (6) is achieved if the identification-relevant motions lie in the null space of ${}^h\bar{\boldsymbol{G}}_r$. This means that the non-redundant directions can be chosen for inducing an identification-relevant motion such that objective (8) is achieved.

Motions $\bar{\dot{\boldsymbol{x}}}_{\mathrm{id}}$ are projected in the null space of ${}^h\bar{\boldsymbol{G}}_r$ by

$$\dot{\boldsymbol{x}}_r^d = ({}^h\bar{\boldsymbol{G}}_r^T)^+ \dot{\boldsymbol{x}}_h^R + (\boldsymbol{I}_6 - ({}^h\bar{\boldsymbol{G}}_r^T)^{+h}\bar{\boldsymbol{G}}_r^T) \boldsymbol{z} , \qquad (28)$$

where $(\boldsymbol{I}_6 - ({}^h\bar{\boldsymbol{G}}_r^T)^{+h}\bar{\boldsymbol{G}}_r^T)$ projects the vector $\boldsymbol{z} \in \mathbb{R}^{n_r}$ in the null space of ${}^h\bar{\boldsymbol{G}}_r$ [15]. The identification motion $\bar{\dot{\boldsymbol{x}}}_{\mathrm{id}}$ is included in $\dot{\boldsymbol{x}}_r^d$ such that $\boldsymbol{N}\dot{\boldsymbol{x}}_r^d = \bar{\dot{\boldsymbol{x}}}_{\mathrm{id}}$ is satisfied, where $\boldsymbol{N} \in \mathbb{R}^{(n_r - n_h) \times n_r}$ contains non-redundant rows of the partial grasp matrix. Replacing $\dot{\boldsymbol{x}}_r^d$ to $\boldsymbol{N}\dot{\boldsymbol{x}}_r^d = \bar{\dot{\boldsymbol{x}}}_{\mathrm{id}}$ yields

$$\boldsymbol{N}({}^h\bar{\boldsymbol{G}}_r^T)^+ \dot{\boldsymbol{x}}_h^R + \boldsymbol{N}\left(\boldsymbol{I}_{n_r} - ({}^h\bar{\boldsymbol{G}}_r^T)^{+h}\bar{\boldsymbol{G}}_r^T\right)\boldsymbol{z} = \bar{\dot{\boldsymbol{x}}}_{\mathrm{id}} , \quad (29)$$

and by solving for $\boldsymbol{z}$, the following is obtained

$$\boldsymbol{z} = \left(\boldsymbol{N}\left(\boldsymbol{I}_{n_r} - ({}^h\bar{\boldsymbol{G}}_r^T)^{+h}\bar{\boldsymbol{G}}_r^T\right)\right)^+ \left(\bar{\dot{\boldsymbol{x}}}_{\mathrm{id}} - \boldsymbol{N}({}^h\bar{\boldsymbol{G}}_r^T)^+ \dot{\boldsymbol{x}}_h^R\right) .$$

After further simplifications, the final expression of $\dot{\boldsymbol{x}}_r^d$ is

$$\dot{\boldsymbol{x}}_r^d = ({}^h\bar{\boldsymbol{G}}_r^T)^+ \dot{\boldsymbol{x}}_h^R \qquad\qquad (30)$$
$$+ (\boldsymbol{N}(\boldsymbol{I}_{n_r} - ({}^h\bar{\boldsymbol{G}}_r^T)^{+h}\bar{\boldsymbol{G}}_r^T))^+ (\bar{\dot{\boldsymbol{x}}}_{\mathrm{id}} - \boldsymbol{N}({}^h\bar{\boldsymbol{G}}_r^T)^+ \dot{\boldsymbol{x}}_h^R) ,$$

where $({}^h\bar{\boldsymbol{G}}_r^T)^+ \dot{\boldsymbol{x}}_h^R$ is responsible for tracking a desired human motion along the redundant directions, and the rest of the expression induces an identification motion, $\bar{\dot{\boldsymbol{x}}}_{\mathrm{id}}$, in the null space of ${}^h\bar{\boldsymbol{G}}_r$.

We discuss the presented strategy through the following illustrative cases:

(i) When a human partner performs only a translational motion, $\dot{\boldsymbol{x}}_h^R$ does not excite the estimator (21). The identification motions $\bar{\dot{\boldsymbol{x}}}_{id}$ induced through (30) are projected in the null space of ${}^h\bar{\boldsymbol{G}}_r$. In this case, $\dot{\boldsymbol{x}}_h^R$ and ${}^h\bar{\boldsymbol{G}}_r$ are as given in the example in (27), and $\boldsymbol{N} = [\boldsymbol{0}_3 \; \boldsymbol{I}_3]$. The identification motion is $\bar{\dot{\boldsymbol{x}}}_{\mathrm{id}} = \boldsymbol{\omega}_{\mathrm{id}}^T$, with $\boldsymbol{\omega}_{\mathrm{id}}$ as the desired angular motion. Eq. (30) yields zero human interaction force and $\boldsymbol{t}_h = -[{}^r\boldsymbol{p}_h]_\times \boldsymbol{f}_r$ since the angular motions of the partners are mutually constrained by the object rigidity.

(ii) When a human performs only angular motions along all directions in $SE(3)$, no further actions taken by the robot towards identification are necessary since $\dot{\boldsymbol{x}}_h^R = \boldsymbol{\omega}_h^T$ already excites the estimator (21) around all directions. In this case, ${}^h\bar{\boldsymbol{G}}_r = [\boldsymbol{0}_3 \; \boldsymbol{I}_3]$, $\boldsymbol{N} = [\boldsymbol{I}_3 \; [{}^r\boldsymbol{p}_h]_\times]$, and $\bar{\dot{\boldsymbol{x}}}_{\mathrm{id}} = \boldsymbol{0}_{3 \times 1}$.

Discussed previously are two extreme cases when the human motions do not contribute towards identification (i), and when the human motions already excite the object dynamics estimator (ii). Any combination of these cases is possible and generically provided by (30).

V. Evaluation

We evaluate the proposed approach in a human-robot cooperative object manipulation setting. We describe the experimental setup, analyze the estimation aspects of (21) and evaluate the effect of the induced identification-relevant motions while taking into account the human desired motion.

A. Experimental setup

The human-robot cooperative object manipulation setting, depicted in Fig. 2, consists of a human partner grasping a handle; a 7 DoF robotic manipulator with an impedance-based controller, enabling the robot compliant behavior, and a low-level joint-space position controller with inverse kinematics, enabling the robot reference trajectory tracking in the task-space; and a manipulated rigid object. The manipulated object is a rectangular wooden plate, with the length, width, and height of $0.56 \times 0.345 \times 0.075$ (m). The robot and the human rigidly grasp the object, which is assured using the coupling mechanisms at both sides, and additional metal pieces for mounting the coupling mechanisms to the object. The true values of the object dynamics are: $m_o = 3.16$ kg for the mass, $^r\boldsymbol{p}_o = [0.324, 0, 0.004]^T$ (m) for the center of mass, and $^r\boldsymbol{J}'_o = [0.0235, 0, 0.005, 0.458, 0, 0.48]^T$ (kg m^2) for the inertia. The center of mass and inertia are only an approximate: the mass distribution is non-homogeneous due to the additional pieces used for coupling. The relative kinematics is $^r\boldsymbol{p}_h = [0.775, 0, 0]^T$ (m) and $^r\boldsymbol{q}_h = [0, 0, 0, 1]^T$; the estimation of relative kinematics, however, can also be incorporated through [6]. The interaction wrenches of both the human and the robot are measured by the 6 DoF JR3 force/torque sensors. The human motion is tracked by the marker-based tracking system Qualisys. The sampling rate of the estimation, control, and wrench acquisition is 1 kHz whereas for the motion tracking it is 0.1 kHz. All measured data is filtered with the Kalman filter to account for the sensor noise.
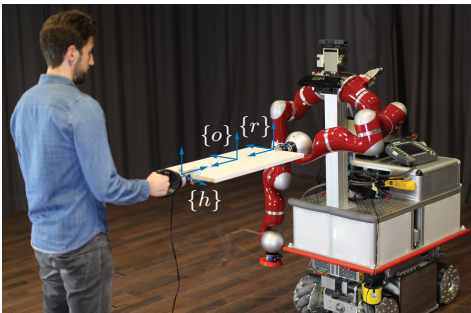
Fig. 2: Human-robot object manipulation experimental setup and frames alignment: x-axis of $\{o\}, \{r\}$ point towards $\{h\}$, x-axis of $\{h\}$ points towards $\{r\}$, z-axes of all frames point upwards, y-axes of all frames complete the right-hand rule.
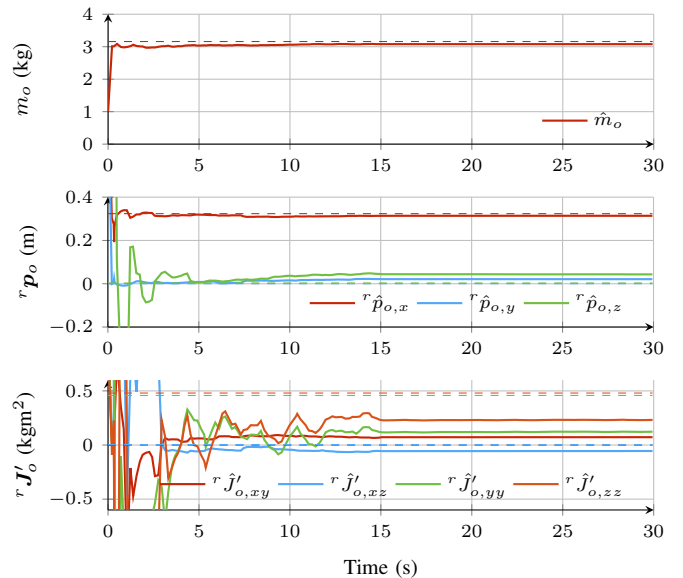
Fig. 3: Estimates of object dynamics: estimated values are plotted with solid lines, and true values with dotted lines. (top) mass estimate $\hat{m}_o$, (middle) center of mass estimates $^r\hat{\boldsymbol{p}}_o$, (bottom) inertia estimates $^r\hat{\boldsymbol{J}}'_o$.

B. Estimation results

The robot induces the identification-relevant motion chosen as $\dot{\boldsymbol{x}}_{\text{id}} = [\boldsymbol{0}_{3\times1}, (\boldsymbol{\omega}_{\text{id}})^T]^T$, where $\boldsymbol{\omega}_{\text{id}} = \frac{\boldsymbol{A}^d}{2} - \boldsymbol{A}^d\text{step}(\boldsymbol{F}^d)$ (rad/s), with the amplitude $\boldsymbol{A}^d = [0.3, 0.15, 0.1]^T$ and frequency $\boldsymbol{F}^d = [0.6, 1.5, 1]^T$, such to satisfy (22). At the first run, the human is instructed not to move, i.e. the human motion is static. The initial values of the estimator are $\hat{\boldsymbol{\theta}}^0 = \boldsymbol{I}_{10\times1}$ and $\boldsymbol{P}^0 = 100\boldsymbol{I}_{10}$. The weighting factor of the estimator is set to $\delta = 0.95$ for $t \in [0, 15]$ (s), and then increased to $\delta = 0.999$ for the rest of the estimation. The results of the online estimation of object dynamics are depicted in Fig. 3. The estimate of $\hat{m}_o$ converges already within $t \approx 6$ ms to $\hat{m}_o = 3.00$ kg, with the relative error of 0.16 kg. At $t \approx 10$ s, the estimate approaches closer to the true value with $\hat{m}_o = 3.06$ kg. At $t_f = 30$ s, the estimated mass is $\hat{m}_0 = 3.08$ kg. The estimate of $^r\hat{\boldsymbol{p}}_o$ converges within $t \approx 5$ s to $^r\hat{\boldsymbol{p}}_o = [0.32, 0, 0]^T$ (m). At t_f, the estimated center of mass is $^r\hat{\boldsymbol{p}}_o = [0.31, 0.02, 0.04]^T$ (m). The relative errors at t_f are: approx. 1 cm along the x-axis, 2 cm along the y-axis, and 4 cm along the z-axis. The four moments of inertia $^r\hat{J}'_{o,xy}, {}^r\hat{J}'_{o,xz}, {}^r\hat{J}'_{o,yy}, {}^r\hat{J}'_{o,zz}$ oscillate during the time interval $t \in [0, 12]$ (s), after which they approach the steady state. The estimates remain within the interval $[-0.05, 0.25]$ for the rest of the estimation time. Similar behavior is manifested for the other inertia parameters, which are omitted due to space restrictions. At t_f, the estimated inertia parameters are $^r\hat{\boldsymbol{J}}'_o = [0.17, 0.07, -0.05, 0.13, 0.01, 0.23]^T$. In general, estimator's performance is affected by the the chosen identification motion induced by the robot as well as the sensor noise appearing in all measurements. The accuracy of $^r\hat{\boldsymbol{p}}_o$ and $^r\hat{\boldsymbol{J}}'_o$ can be improved by choosing $\dot{\boldsymbol{x}}_{\text{id}}$ with

higher amplitudes and frequency (inducing more angular motion). This is especially relevant for the inertia since the values are small. However, robot mechanical limitations prevent us from experimenting with higher robot velocities.

C. Evaluation of the identification motion effect

Evaluation description: We conduct a small user study to evaluate the effect of the induced identification-relevant motions during a human motion. We analyze the performance with 5 human participants, who are instructed to move 0.5 m along the negative y-direction. The desired human motion is required for calculating an equivalent robot motion. However, knowing precisely the human motion poses a challenge on its own [11]. In this work, the human velocity is estimated using the Kalman filter from the human position, acquired by the motion tracking system. This introduces delay in the human motion estimate, resulting in the delayed robot commanded velocities. Such velocities have an influence on subjects, in the form of additional forces acting on the human.

The study consists of evaluating three different conditions, resulting in different robot commanded trajectories. The robot trajectories are either calculated by:

(i) using the proposed approach by inducing the identification-relevant motion $\dot{x}_{\mathrm{id}}$ through (30),

(ii) using a *naive* approach by simply adding the equivalent robot motion (calculated through (15)) and the identification-relevant motion $\dot{x}_{\mathrm{id}}$, i.e. $\dot{x}_{r,\mathrm{naive}} = \dot{x}_r + \dot{x}_{\mathrm{id}}$,

(iii) when no identification-relevant motion is introduced ($\dot{x}_{\mathrm{id}} = \mathbf{0}_{6\times1}$), i.e. following the desired human motion through (15), such to compare the effects of (i) and (ii).

The use of a reference trajectory is motivated by the fact that not all observed forces are undesired due to the delay introduced by the Kalman filter. Each condition is repeated 20 times, totaling in 60 trials per subject; the order of all trials is randomized. The induced identification-relevant motion $\dot{x}_{\mathrm{id}}$ is set as in the previous experiment, with $\mathbf{A}^d = [0.2, 0.15, 0.1]^T$ and frequency $\mathbf{F}^d = [0.33, 0.71, 0.5]^T$. The identification motions slightly differ compared to the first experiment for the safety reasons, discussed subsequently.

Evaluation results: In order to evaluate the influence of the identification motions on the subjects, we analyze the
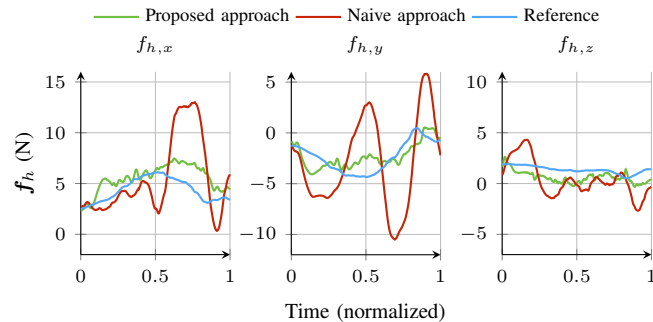
Fig. 4: Mean interaction force of a single subject for all trials: (left to right) force components, $f_{h,x}$, $f_{h,y}$, $f_{h,z}$, for the proposed (green), naive (red), and reference (blue).
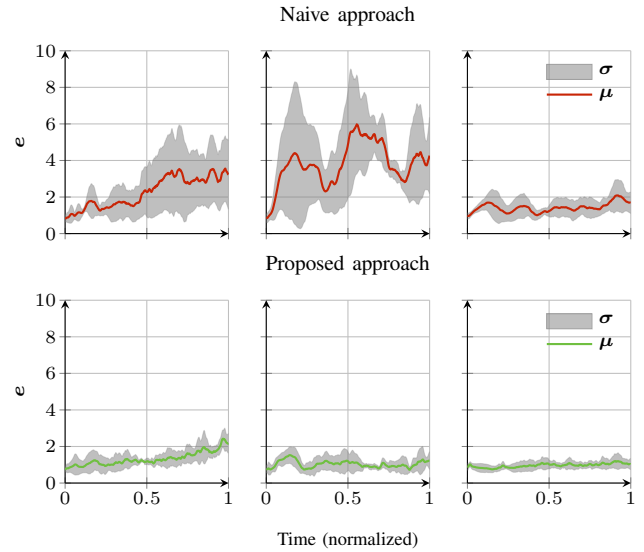
Fig. 5: Interaction error averaged over all trials and subjects: (left to right) mean $\boldsymbol{\mu}$ and variance $\boldsymbol{\sigma}$ along force components $f_{h,x}, f_{h,y}, f_{h,z}$, for the naive (top) and proposed approach (bottom).

interaction forces appearing at the human side. The force measurements are down-sampled to a sequence with fixed length for the rest of the analysis, such to compare the results of different trials. As an example, Fig. 4 depicts the mean of the human interaction force over all trials for a single representative subject, along all axes. The initial insights show a similar profile for the force trajectories obtained when no identification motion is induced (blue) compared to the forces exerted on a subject using the proposed approach (green). This is evident in the force intervals of $[2.3, 7.5]$ in x, $[-4.1, 0.5]$ in y, and $[-0.3, 2.6]$ (N) in z-axis, for the proposed, compared to $[2.5, 6.1]$ for x, $[-4.3, 0.5]$ for y, and $[2.5, 6.1]$ for z-axis, for the reference trajectory across all axes. In the case of the force trajectories obtained using a naive approach (red), the difference in forces with respect to the reference is higher, with values in the intervals $[0.3, 13.0], [-10.5, 5.8], [-2.7, 4.3]$ for all axes, respectively. Particularly, noticeable spikes appear in the force profiles which are undesirable as they disturb the human.

To isolate the effect of undesired interaction and compare the proposed and naive approaches, we define the interaction error as $\boldsymbol{e}(t) = \frac{|\boldsymbol{f}_i(t) - \boldsymbol{\mu}_{\mathrm{ref}}|}{\boldsymbol{\sigma}_{\mathrm{ref}}}$, $\forall i = 1, 2$, where $\boldsymbol{f}_i$ are the human interaction forces of the proposed and naive interaction, respectively, and $\boldsymbol{\mu}_{\mathrm{ref}}$, $\boldsymbol{\sigma}_{\mathrm{ref}}$ are the mean and standard deviation of the reference force $\boldsymbol{f}_{\mathrm{ref}}$ over all trials for a single subject. The error is weighted with the confidence in the desired force, represented by $\boldsymbol{\sigma}_{\mathrm{ref}}$. This enables us to obtain a statistical representation of the undesired interaction for every subject. The resulting interaction error $\boldsymbol{e}$ is then averaged over all trials for each subject. The mean and standard deviation over the averaged interaction errors of all subjects is depicted in Fig. 5. It is evident that the proposed approach reduces the interaction error exerted to the human partner: the mean is $[1.3, 1.0, 1.0]^T$ and the maximum error is $[2.4, 1.5, 1.2]^T$ using the proposed approach, compared

to $[2.3, 3.8, 1.4]^T$ as the mean and $[3.6, 6.0, 2.1]^T$ as the maximum error using the naive approach. The oscillations appearing in the error signals, as well as the high standard deviation using the naive approach, are an indicator of the undesired interaction behavior, caused by the abrupt motions (chosen as $\dot{x}_{id}$), which combined with the physical coupling of the partners, may lead to unstable behavior. The proposed approach shows a drastic improvement compared to the naive approach in terms of interaction error. This is especially relevant as it keeps the team safer since during the study no unstable behavior for the proposed approach is encountered.

The results of this work are applicable to a wider range of applications, where a human and a robot are physically coupled through an object and unknown dynamic parameters exist. The approach is validated using wrench measurements of both interacting partners. Wrench measurements only at the robotic side are not sufficient for accurate dynamics estimation, as those alone do not reflect the external wrenches acting on the object. Available sensing modalities at the human side pose a special challenge in pHRI. Human motion is typically acquired using wearable inertial measurement units or vision-based techniques. Wearable tactile devices (such as tactile gloves [16]) will allow accurate measurements of the human wrenches to be obtained in the foreseeable future. In addition, human wrench could also be estimated using vision approaches, such as [17]. However, such approaches provide only an estimate of the human wrench and any inaccuracies in wrench estimates would be propagated to the dynamics estimator.

VI. CONCLUSION

This paper presents an identification strategy for estimating the unknown dynamic properties of an object in human-robot manipulation tasks. The derived online estimator identifies the object dynamics. We analyze the convergence of the estimator, achieved by satisfying the persistence of excitation condition. We derive identification-relevant motions, which are necessary for parameter identification. By projecting the identification motions into the null space of the partial grasp matrix, relating the human and robot redundant motions, we show that disturbance of the human desired motion is avoided. The proposed approach is experimentally validated in a human-robot cooperative object manipulation setting.

APPENDIX

Expanding the expression of object dynamics model (1), replacing u_o with (4), and solving for wrenches, we obtain

$$^r f_o = m_o \dot{v}_r - m_o g + \dot{\omega}_o \times m_o{}^r p_o + \omega_o \times (\omega_o \times m_o{}^r p_o)$$
$$^r t_o = J_o \dot{\omega}_o + \omega_o \times (J_o \omega_o) - m_o{}^r p_o \times g + m_o{}^r p_o \times \dot{v}_r$$
$$+ m_o{}^r p_o \times (\dot{\omega}_o \times {}^r p_o) + m_o{}^r p_o \times (\omega_o \times (\omega_o \times {}^r p_o)) .$$

Transforming the inertia matrix to the grasping point $\{r\}$ through the parallel axis theorem [18] yields $^r t_o$ as

$$^r t_o = {}^r J_o \dot{\omega}_o + \omega_o \times ({}^r J_o \omega_o) - m_o{}^r p_o \times g + m_o{}^r p_o \times \dot{v}_r .$$

For a vector $a \in \mathbb{R}^3$, matrix $[.a]$ is

$$[.a] = \begin{bmatrix} a_x & a_y & a_z & 0 & 0 & 0 \\ 0 & a_x & 0 & a_y & a_z & 0 \\ 0 & 0 & a_x & 0 & a_y & a_z \end{bmatrix} . \quad (31)$$

REFERENCES

[1] B. Siciliano and O. Khatib, *Springer handbook of robotics*. Springer Science & Business Media, 2008.

[2] M. Lawitzky, A. Moertl, and S. Hirche, "Load sharing in human-robot cooperative manipulation," in *Robot and Human Interactive Communication (RO-MAN), 19th IEEE International Symposium on*, 2010, pp. 185–191.

[3] A. Moertl, M. Lawitzky, A. Kucukyilmaz, M. Sezgin, C. Basdogan, and S. Hirche, "The role of roles: Physical cooperation between humans and robots," *International Journal of Robotics Research*, vol. 31, no. 13, pp. 1657–1675, 2012.

[4] A. Bussy, A. Kheddar, A. Crosnier, and F. Keith, "Human-humanoid haptic joint object transportation case study," in *Intelligent Robots and Systems (IROS), 2012 IEEE/RSJ International Conference on*, 2012, pp. 3633–3638.

[5] A. D. Santis, B. Siciliano, A. D. Luca, and A. Bicchi, "An atlas of physical human-robot interaction," *Mechanism and Machine Theory*, vol. 43, no. 3, pp. 253 – 270, 2008.

[6] D. Cehajic, S. Erhart, and S. Hirche, "Grasp pose estimation in human-robot manipulation tasks using wearable motion sensors," in *Intelligent Robots and Systems (IROS), 2015 IEEE/RSJ International Conference on*, 2015, pp. 1031–1036.

[7] C. G. Atkeson, C. H. An, and J. M. Hollerbach, "Estimation of inertial parameters of manipulator loads and links," *The International Journal of Robotics Research*, vol. 5, no. 3, pp. 101–119, 1986.

[8] P. Dutkiewicz, K. R. Kozlowski, and W. S. Wróblewski, "Experimental identification of robot and load dynamic parameters," in *Control Applications, 2nd IEEE Conference on*. IEEE, 1993, pp. 767–776.

[9] D. Kubus, T. Kroger, and F. Wahl, "On-line estimation of inertial parameters using a recursive total least-squares approach," in *Intelligent Robots and Systems, 2008. IROS 2008. IEEE/RSJ International Conference on*, Sept 2008, pp. 3845–3852.

[10] A. Franchi, A. Petitti, and A. Rizzo, "Decentralized parameter estimation and observation for cooperative mobile manipulation of an unknown load using noisy measurements," in *2015 IEEE Int. Conf. on Robotics and Automation*.

[11] J. Medina, T. Lorenz, and S. Hirche, "Synthesizing anticipatory haptic assistance considering human behavior uncertainty," *Robotics, IEEE Transactions on*, vol. 31, no. 1, pp. 180–190, 2015.

[12] T. Tsuji, P. G. Morasso, K. Goto, and K. Ito, "Human hand impedance characteristics during maintained posture," *Biological cybernetics*, vol. 72, no. 6, pp. 475–485, 1995.

[13] K. J. Astrom and B. Wittenmark, *Adaptive Control*, 2nd ed. Addison-Wesley Longman Publishing Co., Inc., 1994.

[14] S. Ciochina, C. Paleologu, J. Benesty, and A. A. Enescu, "On the influence of the forgetting factor of the rls adaptive filter in system identification," in *Signals, Circuits and Systems, 2009. ISSCS 2009. International Symposium on*. IEEE, 2009, pp. 1–4.

[15] A. A. Maciejewski and C. A. Klein, "Obstacle avoidance for kinematically redundant manipulators in dynamically varying environments," *International Journal of Robotics Research*, vol. 4, pp. 109–117, 1985.

[16] G. Buscher, R. Kiva, C. Schrmann, R. Haschke, and H. Ritter, "Flexible and stretchable fabric-based tactile sensor," *Robotics and Autonomous Systems*, vol. 63, 2015.

[17] T.-H. Pham, A. Kheddar, A. Qammaz, and A. A. Argyros, "Towards force sensing from vision: Observing hand-object interactions to infer manipulation forces," in *Proceedings of the IEEE Conference on Computer Vision and Pattern Recognition*, 2015, pp. 2810–2819.

[18] T. R. Kane and D. A. Levinson, *Dynamics, theory and applications*. McGraw Hill, 1985.